Bioorganic Chemistry 88 (2019) 102936

Contents lists available at ScienceDirect

Bioorganic Chemistry

journal homepage: www.elsevier.com/locate/bioorg

Fluoro-benzimidazole derivatives to cure Alzheimer's disease: *In-silico* studies, synthesis, structure-activity relationship and *in vivo* evaluation for β secretase enzyme inhibition

Sayyad Ali[a,b], Muhammad Hassham Hassan Bin Asad[a,c,*], Soham Maity[b], Wahid Zada[a], Albert A. Rizvanov[c], Jamshed Iqbal[a], Borhan Babak[b], Izhar Hussain[a,*]

[a] Department of Pharmacy, COMSATS University Islamabad, Abbottabad Campus, 22060, Pakistan
[b] Department of Chemistry, Michigan State University, East Lansing, MI 48824, USA
[c] Department of Genetics, Institute of Fundamental Medicine and Biology, Kazan Federal University, 420021, Russia

1. Introduction

Amyloid-β (Aβ) accumulation is linked with the senile neurofibrillary tangles and plaques formation in brain stem lead to Alzheimer's disease (AD). It is composed of 38 to 43 amino acids and produced by the catalytic detachment of Amyloid Precursor Protein (APP) [1]. APP has an amyloid beta encoding domain usually cleaved by a sequence of proteases enzyme called secretases (Fig. 1) [2]. The beta site amyloid precursor protein cleaving enzyme 1 (BACE1 or β-secretase) liberates a soluble *N*-terminus sAPPβ, while γ- secretase producing APP intracellular domain (AICD) and an insoluble Aβ plaques [3]. Aβ-42 is a principal toxic kind of Aβ involved in plaques formation due to the eminent hydrophobicity, accumulation and fibrillization potency that results a delay in clearance and inflammation of the brain [4].

As documented earlier, AD is a progressive neurodegenerative irreparable illness cause of dementia in aged people with high mortality rate [5]. It is marked with a continuous decline in memory, thinking, language, behaviors, judgment, visuospatial, impaired cognitive capability and whole lifestyle. AD is devastating not only for the individual but also for the caretaking family and community [6]. Presently, no absolute treatment is available for AD, however, intended therapeutics used for symptomatical treatment have short-term benefits [1]. The development of medications for AD has been restricted due to the deficit in skills to monitor the advancement in disease, effectiveness of drugs and to approach a conclusive diagnosis at its onset. Though several BACE1 inhibitors were evaluated, however, majority proved ineffective in clinical trials [7]. Peptidic based inhibitors (tetra-decapeptide Lys-Thr-Glu-Glu-Ile-Ser-Glu-Val-Leu-Statine-Val-Ala-Glu-Phe-OH, called STA-200) were proved effective for BACE1 inhibition (IC_{50} = 30.0 nM), however, they were unable to penetrate BBB [8]. Hydroxy ethylene (HE) derivatives of homo-statine (HE bio-isostere) were found previously to produce and mimic BACE1 inhibitory effects (IC_{50} = 1.6 nM) [9]. Similarly, compound KMI-008 (IC_{50} = 413 nM) was documented in literature to decrease 38% sAPPβ load from COS-7 cell-lines, although it was found to overexpress APP moieties [10]. Based on isophthalamide skeleton attached to the small amide isosteres were remained an effective BACE1 inhibitor (IC_{50} = 27.2 nM) [11]. Moreover, family of pyridinyl aminohydantoins-4 derivative was reported to produce an improved pose in S3 domain of BACE1 (IC_{50} = 20 nM) enzyme [12]. Godemann et al. (2009) enlisted below mentioned BACE1 inhibitors, however, proved inadequate to cope AD [13].

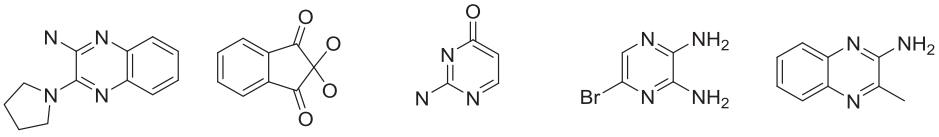

Eli Lilly and Co. introduced LY2886721 after phase-II clinical trial, nevertheless revealed hepatotoxic in nature [14]. Recent failure rate in finding and screening of BACE1 inhibitors has encouraged to continue our efforts in the quest of small molecules (fragments) having therapeutic efficacy for AD. BACE1 inhibitors are meant to arrest Aβ plaques accumulation and to prevent further proliferation of AD. Current advances in computational approaches have been extensively used to

* Corresponding authors at: Department of Genetics, Institute of Fundamental Medicine and Biology, Kazan Federal University, 420021 Kazan, Russia and Department of Pharmacy, COMSATS University Islamabad, Abbottabad Campus, 22060, Pakistan.
E-mail addresses: hasshamasad@cuiatd.edu.pk (M.H.H.B. Asad), Izharhussain@cuiatd.edu.pk (I. Hussain).

https://doi.org/10.1016/j.bioorg.2019.102936
Received 23 November 2018; Received in revised form 7 April 2019; Accepted 15 April 2019
Available online 24 April 2019
0045-2068/

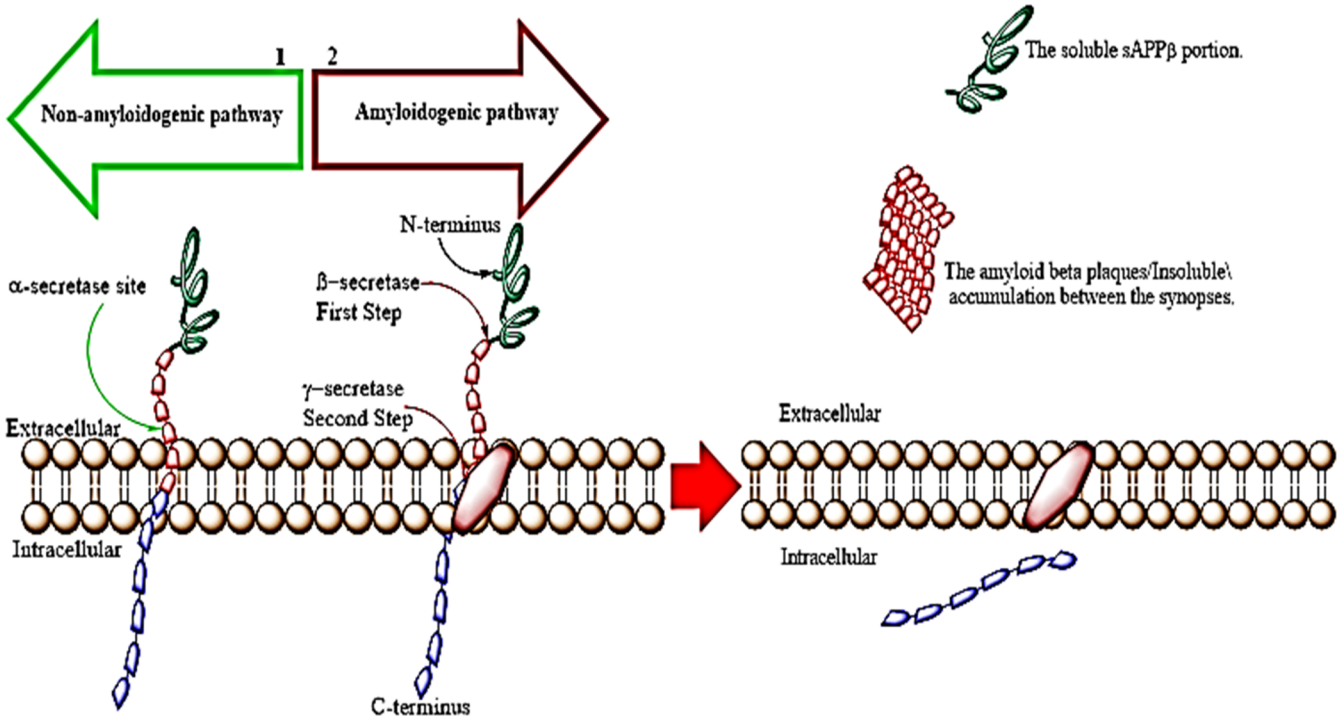

Fig. 1. The APP is initially cleaved by the enzyme β-secretase (BACE1) at the *N*-terminus of the Aβ domain. This cleavage produces the soluble sAPPβ and a C-terminal portion, which experiences a second cleavage by another protease called γ-secretase, which cleaves the transmembrane domain of APP. The final production of Aβ is the main player of the pathogenesis of AD. In the above process β-secretase (BACE1) is rate-limiting enzyme for the initiation of the AD pathogenesis.

discover and optimize novel entities with an affinity for a targeted enzyme. In silico paradigm represents a rich array of possibilities in expediting new targets identification for newly discovered compounds with proposed activity against those target [7]. Virtual screening of enzyme-ligand interaction (docking), synthesis of fluoro-benzimidazole analogs (SAR), βsecretase activity (*in-vitro* assay) and *in-vivo* (animal model) studies was the outlined in the present manuscript.

2. Results and discussion

2.1. Synthesis

The condensation reaction of o-phenylenediamine with the respective substituted aromatic aldehyde resulted in the synthesis of seven compounds (~90% yield) of series of aryl benzimidazoles. The synthesized compounds were given chemical names and assigned codes. These compounds were 2-(4-chlorophenyl)-1H-benzo[*d*]imidazole (**6a**), 2-(4-fluorophenyl)-1H-benzo[*d*]imidazole (**7a**), 2-(2,3,5-trifluorophenyl)-1H-benzo[*d*]imidazole (**7b**), 6-fluoro-2-(2,4,5-trifluorophenyl)-1H-benzo[*d*]imidazole (**7c**), 2-(3-(trifluoromethyl) phenyl)-1H-benzo[*d*]imidazole (**8a**), 6-fluoro-2-(3-(trifluoromethyl) phenyl)-1H-benzo[*d*]imidazole (**8b**), 6-Fluoro-2-(4-(trifluoromethyl) phenyl)-1*H*-benzo[*d*]imidazole (**8c**). Among all 7c was found the most potent, however, ClogP, Lipinski, BBB permeation and IC_{50} was calculated for each compound, and summarized in Table 1. Synthesis of benzimidazoles with more substituted fluorine molecules were 2-(trifluoromethyl)-1H-benzo[*d*]imidazole (**9a**) and 6-fluoro-2-(trifluoromethyl)-1H-benzo[*d*]imidazole (**9b**). Complete detail about their Clog*P*, Lipinski, BBB permeation and IC_{50} is highlighted in Table 2. Table 3 described above mentioned parameters about 6-fluoro-1-(4-fluorobenzyl)-2-(2,4,5-trifluorophenyl)-1*H*-benzo[*d*]imidazole compound (**10a**). Moreover, Table 4 describes detailed NMR information about the structure elucidation of eight benzimidazoles analogs, however, all NMR (^{1}H NMR, ^{13}C NMR and ^{19}F NMR) spectra are available as supplementary material (Figs. 1S – 21S).

2.2. Docking study

Results from molecular docking deduced reliable bonding of benzimidazoles derivatives with the aspartic acid portions (active domain) of BACE1 as shown in Table 5. The most potent compound **7C** was found to pose the best bonding with two key aspartic acids of an active pocket of the BACE1 enzyme. Complete detail about structure of BACE1 and flap region along with optimum polar interaction with the most potent compound **7c** is shown in Fig. 2.

2.3. FRET activity

Benzimidazoles derivatives were found to show different BACE1 inhibitory effects (*in vitro*). Compound **7c** was found the most potent (IC_{50} = 510 nM) and inhibited 98% BACE1 activity at 500 pmol. **6a** was noted the least potent among all having IC_{50} = 312.3 μM with 39% inhibitory effect of the same concentration. Rest of all compounds **9a** (IC_{50} = 1.3 μM, 72% inhibition), **10a** (IC_{50} = 5.6 μM, 65% inhibition), **8a** (IC_{50} = 15.3 μM, 57% inhibition), **8b** (IC_{50} = 19.5 μM, 52% inhibition), **7b** (IC_{50} = 93.3 μM, 55% inhibition), **7a** (IC_{50} = 112.3 μM, 80% inhibition), **9b** (IC_{50} = 117.3 μM, 58% inhibition), **8c** (IC_{50} = 123.7 μM, 60% inhibition) were found in between in efficiency. A complete list of compounds is mentioned in Tables 1–3 along with their chemical names, structures and IC_{50} values.

2.4. Morris water maze assay

In vivo studies designed to map out the efficacy of newly synthesized compounds via behavioral tests. Morris water maze assay showed that aluminum chloride inducted neurotoxicity to the mice exhibited raised escape latency (35.70 ± 3.95) in comparison to the control mice (15.60 ± 1.01) on the fifth day. The treated mice showed improved learning curves and animals showed better spatial learning and memory (20.99 ± 3.56; $p < 0.05$) when compared to the $AlCl_3$ treated group. The compound **7c** treated mice took more time during exploring the

Table 1
Represents the synthesis of benzimidazoles derivatives from $NaHSO_3$ and o-phenylenediamine/halo-o-phenylenediamine with different aromatic aldehydes in presence of DMF at 80 °C resulted in impressive yield of compounds with their IC_{50} values.

Code	Diamine	Fluro-aryl-aldehyde	Product (% yield)	ClogP, (Lipinski), BBB permeation, (other parameters)	IC_{50} BACE1
6a			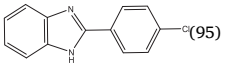 (95)	3.75, 0 violation, Yes (Highly absorbed by GIT; HB_Donor: 1; HB_acceptor: 1)	313.3 μM
7a			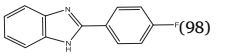 (98)	3.25, 0 violation, Yes (Highly absorbed by GIT; HB_Donor: 1; HB_acceptor: 2)	112.3 μM
7b			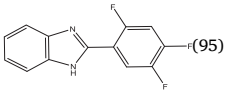 (95)	3.89, 0 violation, Yes (Highly absorbed by GIT; HB_Donor: 1; HB_acceptor: 4)	93.3 μM
7c	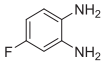		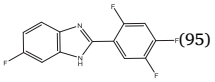 (95)	4.11, 0 violation, Yes (Highly absorbed by GIT; HB_Donor: 1; HB_acceptor: 5)	510 nM
8a		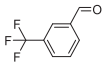	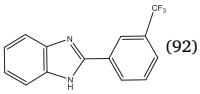 (92)	3.96, 0 violation, Yes (Highly absorbed by GIT; HB_Donor: 1; HB_acceptor: 4)	15.5 μM
8b	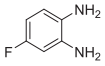	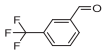	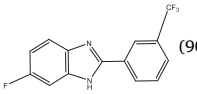 (90)	4.23, 0 violation, Yes (Highly absorbed by GIT; HB_Donor: 1; HB_acceptor: 5)	19.5 μM
8C	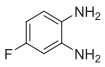	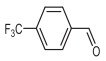	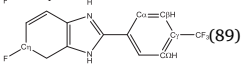 (89)	2.20, 1 Violation, No, (Highly absorbed by GIT; HB_Donor: 1; HB_acceptor: 5)	123.7 μM

target quadrant (31.10 ± 1.23) than the $AlCl_3$ models. The Alzheimer's models crossed the said quadrant (5.23 ± 1.13) and the control has crossed quite often the quadrant as compare to (12.43 ± 1.87) and the treated animal with our synthesized compound gave results in between the two described groups (9.32 ± 1.24). Overall results are expressed in Fig. 3.

2.5. Novel object recognition assay

Novel object recognition assay demonstrated no significant difference in time spent by the mice in exploring of two identical objects in the training session. In the testing phase, the negative control mice explored the novel object for a longer time period with recognition test (RT) (67%) while positive control (AD model) and AD-mice treated with the synthesized compounds showed a considerably lower RT value at 45.8% and 57% respectively (Fig. 4). The average exploration time and the recognition index was indicated significant at $p < 0.0002$, however, **7c** was found the best to enhance the three-dimensional spatial learning/memory of $AlCl_3$ induced model at $p < 0.05$.

Proteases BACE1 (β-secretase) is attributed for amyloid beta peptide (Aβ42) formation led to senile plaques accumulation common in Alzheimer's disease [15]. BACE1 is more prone to produce Aβ42 at all level of the nervous system [16]. Being a substrate for BACE1 APP led to rapid proteolytic action end up with the progression of AD. These circumstances reinforced the amyloid cascade hypothesis and propose BACE1 as a potential therapeutic target. Several attempts were made previously to develop computationally or synthesized BACE1 inhibitors, however, a dire need has been felt nowadays [17]. Active domain of BACE1 is huge, open, lipophilic and possess flexible conformation usually holds a flexible β-hairpin loop (67–77 residues flap-region) to position the substrate for catalytic activity of an enzyme optimally [18,19]. BACE1 inhibitors have rigid hydrogen bonding framework which occupied S1 to S3 binding domain and found to involve in essential H-bonding along with hydrophobic-interactions. Perhaps **7c** showed inhibitory potential by following this principle (Fig. 2) which accurately docked within the specified flexible binding domain. Backbone movements of the potential ligand(s) was due to the energy minimization to reduce the intrinsic property of rigidity of both the

Table 3
Represents the synthesis of 6-fluoro-1-(4-fluorobenzyl)-2-(2,4,5-trifluorophenyl)-1*H*-benzo[*d*]imidazole with benzyl chloride along with IC_{50} value.

Code	Benzimidazole derivative	Product	% Yield	ClogP, (Lipinski), BBB permeation	IC_{50} BACE1
10a	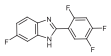	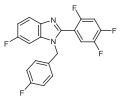	88	3.90, 1 violation, No, (Lowly absorbed by GIT; HB_Donor: 0; HB_acceptor: 6)	5.6 μM

Table 2
Represents the synthesis of benzimidazoles with substituted fluorine molecules with their IC $_{50}$ values.

Code	Diamine	Product	% Yield	ClogP, (Lipinski), BBB permeation	IC_{50} BACE1
9a	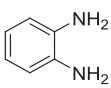	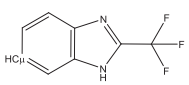	95	2.98, 0 violation, Yes, (Highly absorbed by GIT; HB_Donor: 1; HB_acceptor: 4)	1.3 μM
9b	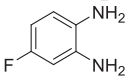	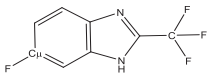	88	2.30, 0 violation, Yes, (Highly absorbed by GIT; HB_Donor: 1; HB_acceptor: 5)	117.3 μM

Table 4
Detailed NMR spectroscopic description to configure structures of newly synthesized compounds.

Sr. No	Code of compound	Compound name	Spectroscopic detail
1	6a	2-(4-chlorophenyl)-1H-benzo[*d*]imidazole	Yield: 95%, Column chromatography [Ethylacetate:hexane (1:9), R*f* = 0.8]; **^{1}H NMR** (500 MHz, DMSO-d_6): δ 11.20 (1H, s), 7.7 (2H, dd, J = 7 Hz), 7.15 (2H, d, J = 7 Hz), 6.9 (2H, dd, J = 7.8 Hz), 6.6 (2H, d, J = 7.8 Hz); **^{13}C NMR** (125 MHz, DMSO-d_6): δ 150.1, 143.4 (2C), 131.6 (2C), 133.6 (2C), 130.6 (2C), 123.2 (2C), 123.2 (2C); **HR-EI MS**: m/z 228.04539; [(M + 1)$^+$ Calcd for $C_{13}H_9ClN_2$ 228.04543]
2	7a	2-(2,3,5-trifluorophenyl)-1H-benzo[*d*]imidazole	Yield: 98%, Column chromatography [Ethylacetate:hexane (1:9), R*f* = 0.9]; **^{1}H NMR** (500 MHz, DMSO-d_6): δ 10.5 (1H, s), 7.5 (4H, q), 7.1 (4H, q); **^{13}C NMR** (125 MHz, DMSO): δ 167.7 (d $J_{C\text{-}F}$ = 58.2 Hz), 156.0, 142.6 (2C), 134.4, 128.0 (2C), 121.6 (2C), 116.6 (4C); **^{19}F NMR** (470 MHz, DMSO-d_6): δ −60.1; **HR-EI MS**: m/z 212.07492; [(M + 1)$^+$ Calcd for $C_{13}H_9FN_2$ 212.07498]
3	7b	2-(2,3,5-trifluorophenyl)-1H-benzo[*d*]imidazole	Yield: 98%, Column chromatography [Ethylacetate:hexane (0.5:9.5), R*f* = 0.9]; **^{1}H NMR** (500 MHz, DMSO-d_6): δ 12.4 (1H, s), 8.2 (1H, q), 7.8 (1H, q), 7.7 (1H, d, J = 7.5 Hz), 7.6 (1H,d, J = 8 Hz), 7.2 (2H, q); **^{13}C NMR** (125 MHz, DMSO): δ 169.9, 169.2, 161.2, 154.6 (2C), 144.3 (2C), 133.5, 124.4 (2C), 109.8 (3C); **HR-EI MS**: m/z 266.04667; [(M + 1)$^+$ Calcd for $C_{13}H_7F_3N_2$ 266.04671]
4	7c	5-fluoro-2-(2,3,5-trifluorophenyl)-1H-benzo[*d*] imidazole	Yield: 95%, Column chromatography [Ethylacetate:hexane (1:9), R*f* = 0.85]; **^{1}H NMR** (500 MHz, DMSO-d_6): δ 12.5 (1H, NH, s), 7.9 (1H, d, J = 8.65 Hz), 7.6 (1H, d, J = 7 Hz), 7.4 (1H, s), 7.2 (1H, d, J = 4.5 Hz), 6.9 (1H, t, J = 9 Hz); **^{13}C NMR** (175 MHz, DMSO-d_6): δ 140.5(1C), 128.6 (1C), 127.6 (1C), 124.5(1C); **^{19}F NMR** (500 MHz, DMSO-d_6) δ −115.0 (2C), −131.0, −141.7; HR-EI MS: m/z 266.04665; [(M + 1) + Calcd for $C_{13}H_6F_4N_2$ 266.04671]
5	8a	2-(3-(trifluoromethyl) phenyl)-1H-benzo[*d*] imidazole	Yield: 92%, Column chromatography [Ethylacetate:hexane (1:9), R*f* = 0.8]; **^{1}H NMR** (500 MHz, DMSO-d_6): δ 12.4 (1H, NH, s), 8.5 (2H, t, J = 7.5 Hz), 8.0 (1H, s), 7.7 (2H, s), 7.3 (2H, t, J = 3 Hz), 5.8 (1H, s); **^{13}C NMR** (175 MHz, DMSO-d_6): δ 162.3, 149.6, 142.5 (2C), 133.7, 131.1, 130.2, 129.9, 128.5 (d, J = 272.8 Hz), 126.2 (2C, d, J = 3.2 Hz), 122.8, 122.5 117.4, 113.4; **^{19}F NMR** (470 MHz, DMSO-d_6) δ −61.3; HR-EI MS: m/z 262.07172; [(M + 1) + Calcd for $C_{14}H_9F_3N_2$ 262.07178]
6	8b	5-fluoro-2-(3-(trifluoromethyl) phenyl)-1H-benzo[*d*]imidazole	Yield: 90%, Column chromatography [Ethylacetate:hexane (1:9), R*f* = 0.92]; **^{1}H NMR** (500 MHz, DMSO-d_6): δ 11.2 (1H, NH, s), 8.2 (1H, t, J = 8 Hz), 8.0 (1H, s), 7.5 (1H, s), 7.4 (1H, t, J = 10 Hz), 7.1 (1H, s), 6.9 (1H, t, J = 7.5 Hz), 5.2 (1H, s); **^{19}F NMR** (470 MHz, DMSO-d_6) δ −61.3, −120.9; HR-EI MS: m/z 280.06228; [(M + 1) + Calcd for $C_{14}H_8F_4N_2$ 280.06236]
7	8c	6-Fluoro-2-(4-(trifluoromethyl)phenyl)-1*H*-benzo[*d*]imidazole	Yield: 88%, Column chromatography [Ethylacetate:hexane (1:9), R*f* = 0.9]; **^{1}H NMR** (500 MHz, DMSO-d_6): δ 12.5 (1H, NH, s), 8.2 (1H, s), 8.2 (1H, d, J = 8 Hz), 8.0 (1H, s), 7.5 (2H, m), 7.2 (1H, t, J = 8 Hz), 6.9 (1H, m); **^{19}F NMR** (470 MHz,DMSO-d_6) δ −62.9, −119.9; HR-EI MS: m/z 280.06228; [(M + 1) + Calcd for $C_{14}H_8F_4N_2$ 280.06236]
8	9a	2-(trifluoromethyl)-1H-benzo[*d*]imidazole	Yield: 95%, Column chromatography [Ethylacetate:hexane (2:8), R*f* = 0.8]; **^{1}H NMR** (500 MHz, DMSO-d_6) δ 13.2 (1H, NH, s), 7.71 (2H, t, J = 2.5 Hz), 7.3 (2H, d, J = 7.5 Hz); **^{19}F NMR** (470 MHz, DMSO-d_6): δ −119.2; HR-EI MS: m/z 204.03099; [(M + 1) + Calcd for $C_7H_5F_3N_2$ 204.03106]
9	9b	5-fluoro-2-(trifluoromethyl)-1H-benzo[*d*] imidazole	Yield: 88%, Column chromatography [Ethylacetate:hexane (2:8), R*f* = 0.85]; **^{1}H NMR** (500 MHz, DMSO-d_6): δ 11.3 (1H, NH, s), 7.7 (1H, q), 7.5 (1H, d, J = 8.5 Hz), 7.2 (1H, td. J = 2 Hz); **^{19}F NMR** (470 MHz,DMSO-d_6) δ −62.9, −75.1; HR-EI MS: m/z 204.03099; [(M + 1) + Calcd for $C_7H_4F_4N_2$ 204.03106]
10	10a	6-Fluoro-1-(4-fluorobenzyl)-2-(2,3,5-trifluorophenyl)-1*H*-benzo[*d*]imidazole	Yield: 88%, Column chromatography [Ethylacetate:hexane (1:9), R*f* = 0.8]; **^{1}H NMR** (500 MHz, DMSO-d_6): δ 12.6 (1H, NH, s), 8.2 (1H, m), 7.8 (1H, m), 7.7 (1H, d. J = 8 Hz), 7.6 (1H, d. J = 8 Hz), 7.2 (5H, m); **^{19}F -NMR** (470 MHz,DMSO-d_6) δ −116.5, −132.1, −142.8; HR-EI MS: m/z 374.08417; [(M + 1) + Calcd for $C_{20}H_{11}F_5N_2$ 374.08424]

Note: Abbreviations used to interpret NMR spectra were: s, singlet; dd, doublet of doublets; m, multiplet; d, doublet; t, triplet; q, quartet; quint, br.t, broad triplet; quint, quintet; sep, septet; dist., distorted; sex, sextet.

moieties [20]. Optimum polar interaction with both of the catalytic aspartates (Asp32 & Asp 228) aligned the benzimidazole scaffold toward S2 therefore bound via van der Waals interactions with Val 69, Ile126 and Tyr 198 amino acids. Overall geometry, posing of scaffold and optimum polar interaction within the active domain of **7c** conferred it as a lead to explore as a targeted BACE1 inhibitor [20]. Molecular docking described in detail about compound '**7c**' from lowest possible energy level to the higher state in bound form. Optimum binding energy with aspartate at the catalytic domain was observed at the lowest energy level. Lower optimum binding led to better bioactivity along with strong polar interaction. No substantial deviation was observed from first one and lower possible energy binding pose when compared with root means square deviation lower bonded (rmsd l.b) value equal to zero. Compound **7c** had optimum binding at others poses above rank 01 and were proved parallel *in-silico* and *in-vitro* studies (Tables S1–S2) [21].

Present article enlisted ten synthesized compounds treated against BACE1 enzyme. Structure activity relationship based on the data-set was developed. Substitution of hydrogen atom with chlorine at Cγ showed significant inhibitory activity. Fluorine for molecular mechanics calculations and in docking was adopted based on fluorine chemistry which has tremendous role in creation of effective BACE1 inhibitors besides US patent [US15751765] [22]. Attachment of fluorine at the aldehyde ring successfully enhanced the activity along with marked bioavailability at the target site (**7a** & **7b**). Introduction of an extra fluorine atom on diamine nucleus conferred more potent enzyme inhibition [17,23]. A marked decline in activity was observed with -CF3 moiety when shifted from Cβ to Cγ along with poor blood brain barrier penetration value. Attached of trifluoro- moiety to the benzimidazole ring led to optimum activity for BACE1 inhibition. Inserting fluorine atoms on the benzene or carbon atom as in case of **7c** gave us pretty remarkable results (bioavailability enhanced at the target site depicted by the virtual screening) [23,24]. The most active compound **7c** was reacted with 4-fluorobenzyl chloride while resulted product was unable to show optimum attachment with aspartate, however, *in vitro* results were more promising. The molecular docking results showed that the ligand that already contained the two aryl groups had a versatile level of inhibitory activity with different

Table 5
Bonding of benzimidazoles derivatives with the aspartic acid (active domain) of BACE1, depicted as in red sticks, generated from AutoDock Vina and MOE molecular docking software.

Codes	Ligand shown in the active(red) pocket of the entire enzyme.	Ligand surrounded by amino acids including the active members(aspartic acid 32/and 228)	The active domain is more highlighted as b elow with bonds
7a	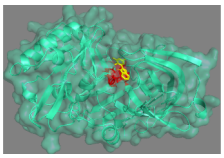	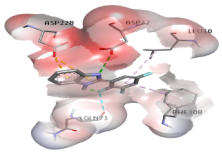	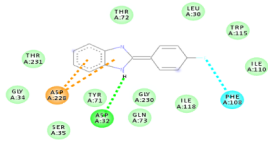
7c	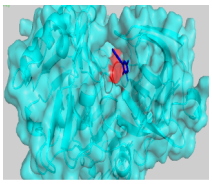	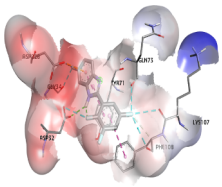	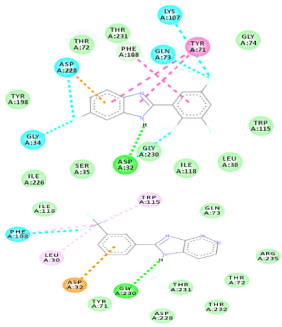
8a	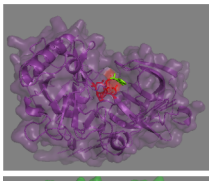	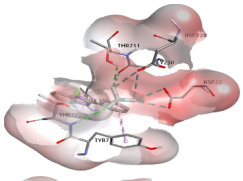	
8b	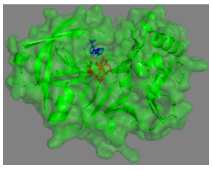	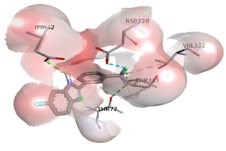	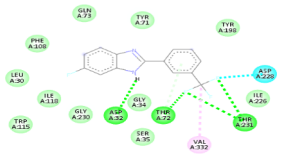
8c	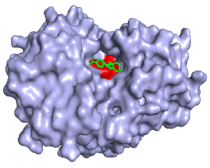	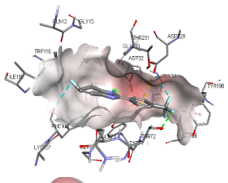	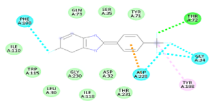
9a	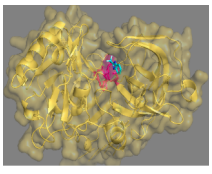	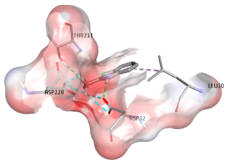	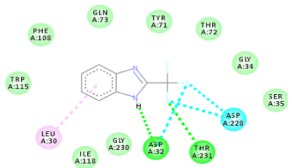
9b	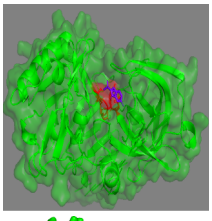	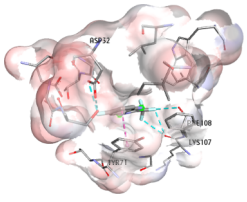	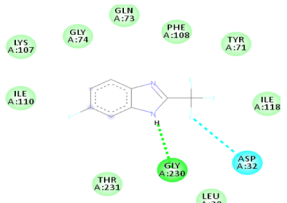
10a	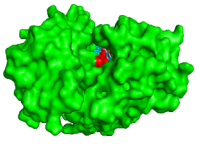	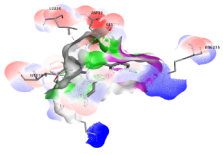	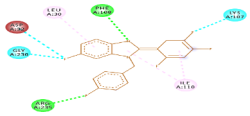

numbers/and positions with the attached fluorine moieties [24,25].

Morris water maze test remained as a typical technique for studying the spatial memory/learning in rodents and is generally applied to examine the deficits in behaviors in AD animal models. Despite this, launching the water maze experiment in precise infective agents' free environment is a complex technique, the screening circumstance is rather stress-inducing to the rodents. A less complicated and more favorable behavioral test might be more help-full to assess a huge quantity of possibly useful compounds in AD rodents. The novel object recognition test is founded on the learned instinct of mice to find out/explore novelty/ unfamiliarity and is a complete working memory test (Fig. 5) [26]. Both human and animals have hippocampus involved in the formation of recognition memory. Novel object recognition test does not need spatial exploration/learning and demand for a positive or negative stimulus. Such stimuli might be the cause of stress in mice and this stress has been concluded as a chief factor negatively affecting the

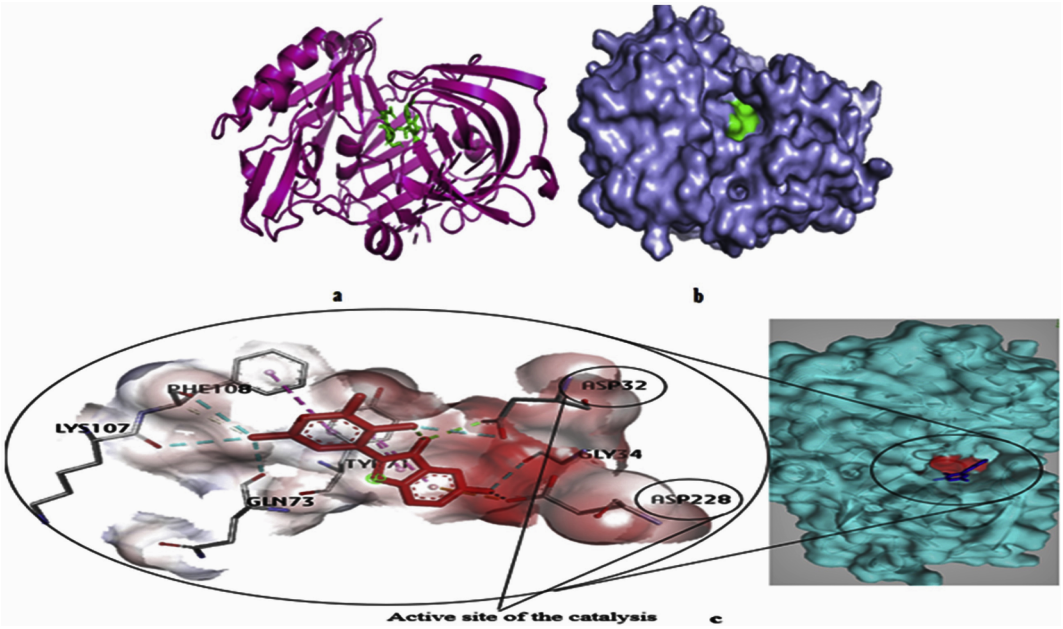

Fig. 2. Describes in detail the structure of BACE1 and flap region (a) along with optimum polar interaction with potential compound **7c** (b). Enhanced view of polar interaction with the most potent compound **7c** is highlighted (c).

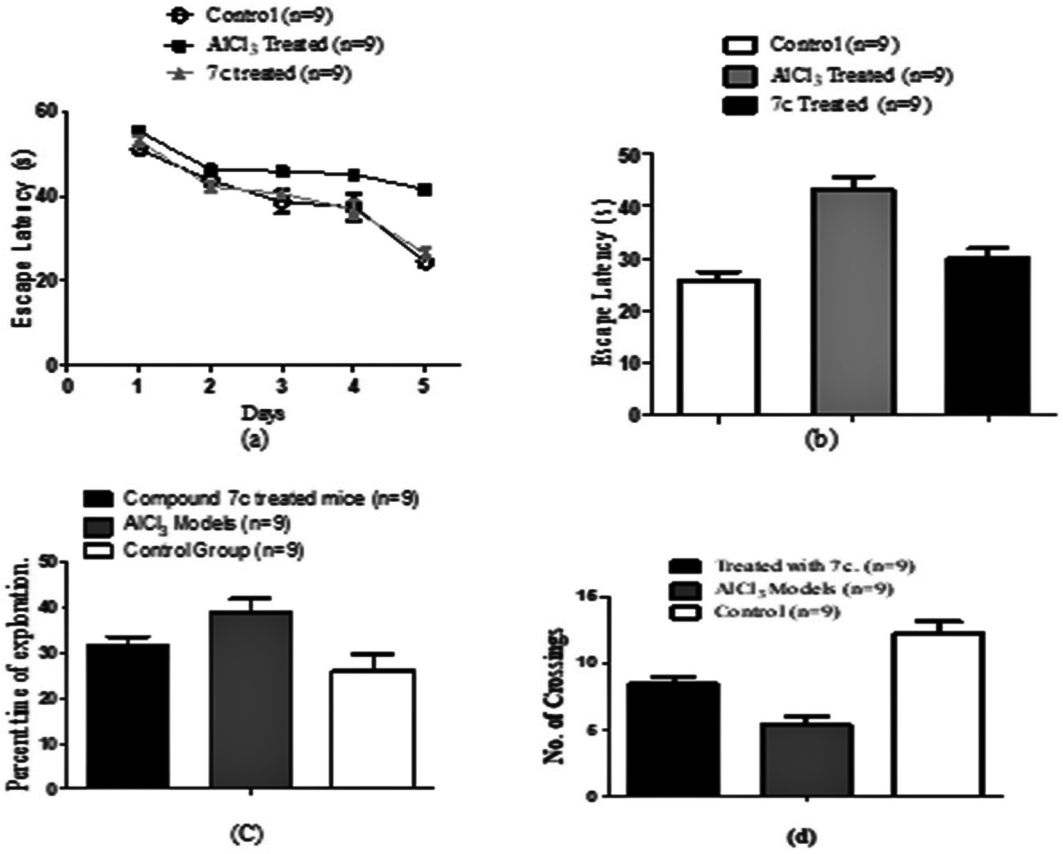

Fig. 3. The results of compound 7c on the memory and learning on mice models exploiting the Morris water maze screening assay. (a) Escape latency time to reach the platform on various days of the $AlCl_3$ induced neurotoxicity group, the control, and compound 7c treated group, (b) represent the fifth-day trials comparison studies among the three groups. (c) Represent the percent total time the rodent spends in the explorations of the target quadrant and similarly (d) shows how many times the mice crossed target quadrant.

learning and memory [27]. Keeping in view all the physiological relevancy in mind this test has been carried out for compound **7C** potentially beneficial for *in-vitro* evaluations [28].

3. Conclusions

The present study described the synthesis of eight fluoro-benzimidazole derivatives relayed on virtual screening as a BACE1 inhibitor, in particular,

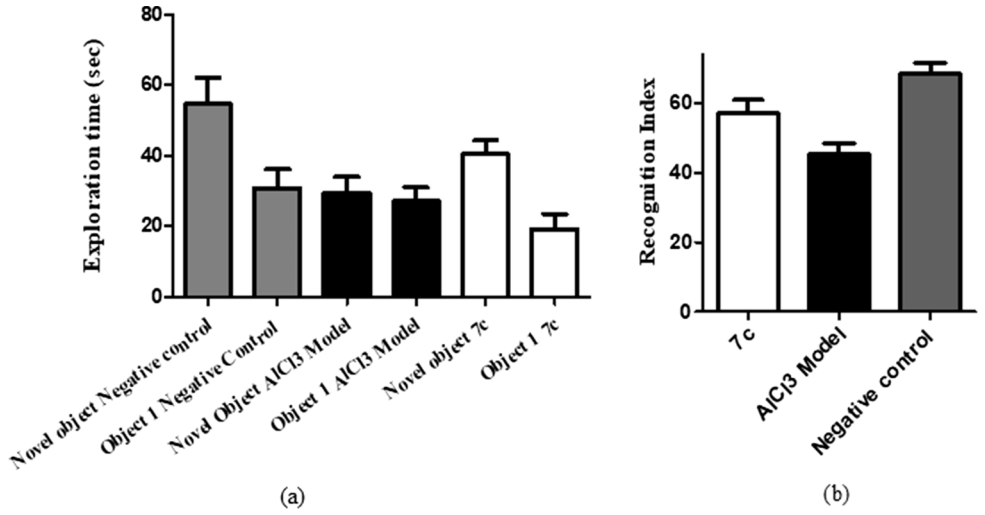

Fig. 4. Novel object recognition assay: Synthesized compound 7c enhanced the three-dimensional spatial learning/memory of $AlCl_3$ induced model.

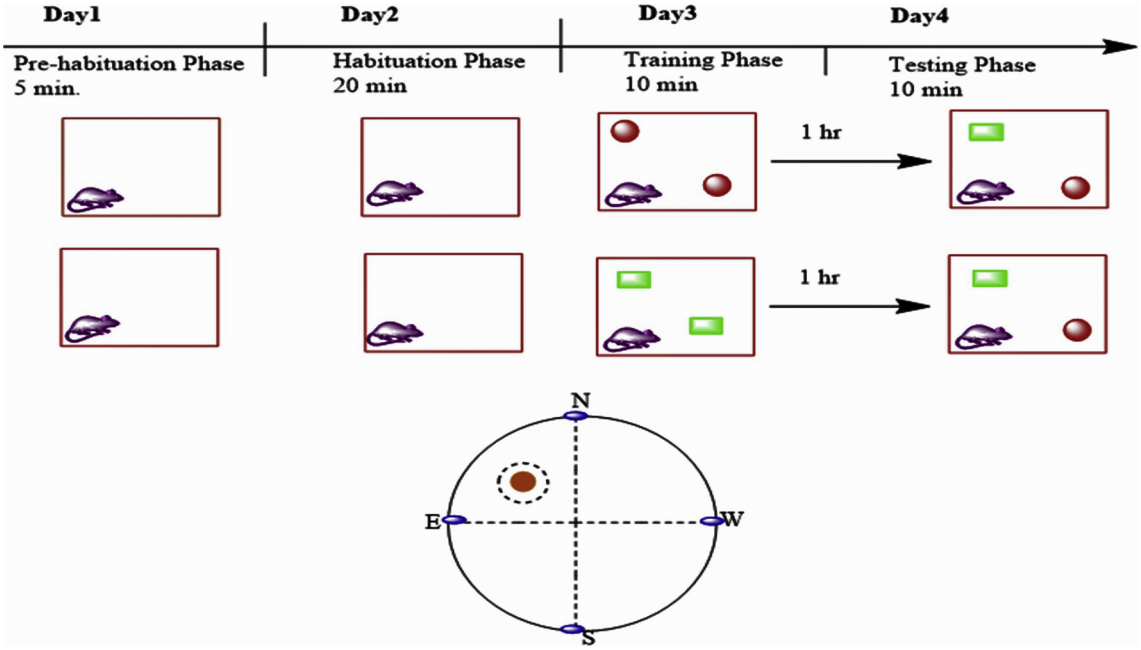

Fig. 5. A diagrammatic illustration of the novel object recognition test. A pre-habituation and habituation phases followed by a pair of objects located in the empty boxes (10 min training session). Mice were put in the experimental field having familiar and unfamiliar (novel) objects after 60 min. Time was noted for exploring the objects and for each object by the mice (video recording).

the most potent and effective 6-fluoro-2-(2,4,5-trifluorophenyl)-1H-benzo [*d*]imidazole (**7c**). Attachment of fluorine on the carbon (benzene/aldehyde/benzimidazole ring) led to the improved potency of the moieties and also sometimes resulted in enhanced bioavailability at the target site. Optimized *in-silico* results have been validated by the *in-vitro* and *in-vivo* results which showed the arrest of the Aβ plaques with varying *in-vitro* IC_{50} results, and an orally bioactive brain-penetrating inhibitor that effectively reduced the AD symptoms in mice models. Additional changes to this series intended to improve the pharmacological activities and reduce the off-target adverse reactions would be the focus of the future research.

4. Material and methods

4.1. Virtual screening with molecular docking

Benzimidazole fragment synthesizes after thoroughly *in silico* authentication. For all β-secretase inhibitors, molecular docking was done using MGL tools v1.5.6 and AutoDock v4.2. ChemDraw ultra 16.0 was used to draw the structures, subsequently converted to the 3D via chem-3D pro 16.0. Moreover, energies of the ligand structures were minimized with MM2. The β-secretase (PDB ID: 1FKN) was downloaded from RCSB protein data bank in less than 2.0 Å resolution. Addition of water, charges, hydrogen atom along with the removal of co-crystallized ligand, protein structures were prepared for molecular docking. AutoDock vina exploits the Gasteiger partial charges estimation technique for conformers of protein calculations to ligand was adopted. Similarly, the ligands were added with Gasteiger charges and all the rotatable bonds were determined based on the ligand molecules [18]. Active site was specified via grids around the co-crystallized ligands before the removal of ligands. For the sake of docking, nine poses of the compound were generated via Lamarkian Genetic Algorithm. The possible binding sites and docked poses were selected visualizing and binding free energies. PyMol tool v2.1 and similarly visualizer discovery studio v17.2 was used to acquire the possible binding pose

figure [29]. The ligand-enzyme interaction was redocked and authenticate via Molecular Operating Environment (MOE) drug discovery software by Chemical Computing group and similarly the pharmacokinetic properties of the ligand i.e. Clog*P*, (Lipinski), BBB permeation were calculated through MOE [30].

4.2. Synthesis of benzimidazoles derivatives

Based on the *in-silico* screening, a series of eight different benzimidazoles were synthesized. The reactants and all the reagents were purchased from Sigma Aldrich and Alfa Aesar. Several approaches are available for the chemical synthesis of derivatives of benzimidazole [31]. For the synthesis of 2-substituted benzimidazoles two approaches were used;

(a). Synthesis of 2-aryl benzimidazoles was done by the condensation reaction of o-phenylenediamine with the respective substituted aromatic aldehyde in the presence of $NaHSO_3$. An equimolar concentration of 0.5 mmol of *ortho*-phenylenediamine and the respective aryl-aldehyde 0.5 mmol were systematically mixed in 2 ml of DMF along with (0.15) mmol of sodium hydrogen sulphite. The reaction mixture was stirred at 80 °C until completed and checked periodically with TLCs. By adding 20 ml of distilled water (with constant stir) the mixture was cooled at room temperature. The product was formed and separated as free-floating solid. It was accumulated by suction filtration, washed with distilled water and finally dried. The gummy solid material was extracted with ethyl acetate and washed with water and brine solution. It was dried on sodium sulphate and the final residue was extracted with a column on silica gel by using hexane: ethyl acetate (2–6:1–3) as eluent [32]. The overall reaction for the synthesis of 2-Aryl-substituted benzimidazoles is given below.

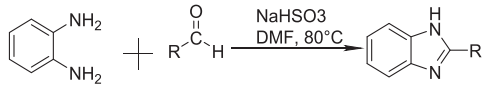

(b). Ortho-phenylenediamine was mixed with trifluoroacetic acid (TFA) at an equimolar concentration of 0.5 M, at a reaction temperature of 70 °C for 2 h. The excess TFA was evaporated to get the desired product in a sufficient quantity/yield. The product was made purified by a silica gel chromatography column to obtain total free analytical yield (overall reaction is given below) [33].

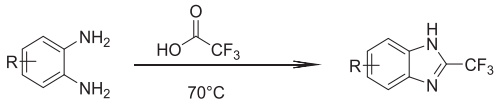

(c) 5-Fluoro-2-(2,3,5-trifluorophenyl)-1*H*-benzo[*d*]imidazole (1 M) was added to round bottom flask having acetone (30 ml) along with catalytic amount of triethylamine (10–15 drops) and stir for half an hour under reflux condition followed by addition of 4-fluorobenzyl chloride equimolar compared to the imidazole in the reaction mixture. After 8 h, the final product was confirmed through TLC and were purified through column chromatography through silica gel.

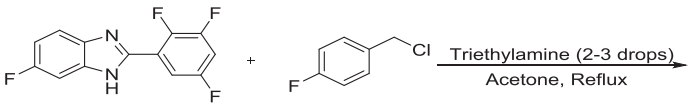

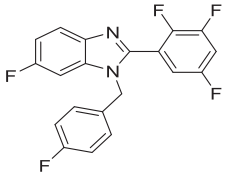

4.3. Spectral analysis

The ^{1}H NMR, ^{13}C NMR, and ^{19}F NMR spectra were recorded by Agilent (DDR2 500 MHz NMR spectrometers) equipped with 7600AS 96 sample autosamplers running VnmrJ 3.2A. The instruments have TMS as internal standards. The values of the chemical shift were described in ppm (δ) units and the coupling constants (*J*) were recorded in MHz.

4.4. Fluorescence resonance energy transfer (FRET) assay

BACE1 blocking activity for newly synthesized benzo[*d*]imidazole derivatives was performed via Sigma –Aldrich FRET-based screening assay activity kit (product # CS0010).

Briefly, assays were performed in a total 100 µl volume composed of BACE1 substrate (20 µl, 50 µM, Catalog # A1472), fluorescent assay buffer (78 µl/78-X µl, pH 4.5, catalog # F8303), test samples (X µl, 100 µM) and BACE1 enzyme (2 µl, ~0.3 unit/µl, Catalog # B9059) in 96 well plate reaction mixture incubated at 37 °C for 1:15 min at optimized assay condition (usually 5%-20% fluorescent product produced from substrate within 1–2 h). Baseline fluorescence reading (time zero reading) was noted immediately after the addition of BACE1 enzyme (fluorometer with excitation at 320 nm) while emission signal was read at 405 nm room temperature. Both BACE1 substrate and enzyme were prepared in the buffer, while tested samples were initially dissolved in DMSO (5%) subsequently serially diluted with provided buffer in the desired volume (2 µl, 3 µl & 5 µl) and strength (200 pmol, 300 pmol & 500 pmol) respectively. A standard curve was generated between fluorescent unit (FU) against standard (100 µM, 1–5 µl) solution concentration (100–500 pmol) to find out 50% BACE1 cleavage. FU of the blank was subtracted from all signal readings of the reaction mixtures. Sample blank (buffer & substrate) was treated as a negative control, however, positive control was a sample (buffer & substrate) with enzyme mixture (www.sigmaaldrich.com). IC_{50} of each of the tested compounds were compared and calculated using GraphPad Prizm v5 software.

4.5. In vivo study

4.5.1. Experimental animals

All the experiments were conducted using male BALB/c mice arranged from NIH (Islamabad, Pakistan). Animals housing was in standard Type III cages of Makrolon TM in a group of 3 or 4 mice with bedding of sawdust. Water and food were supplied ad libitum, water was thoroughly been checked and freshly supplied on daily basis to prevent infectious agents' growth, similarly, sawdust bed was periodically checked and replaced to prevent all the possible infective organisms results from mice' feces. All animals were divided into six groups, each group (n = 9) were between 3 and 5 months of age.

4.5.2. Animal preparation for behavioral tests

Animals were given drinking water with aluminum chloride (17 mg/kg) for a period of 32 days as a positive control while the negative control group was provided with normal tap water. Treated animals were given synthesized compound (50 mg/Kg) with $AlCl_3$. Morris Water Maze test trials were carried out from day 27th to day 31st per oral treatment, whereas the remaining behavioral tests were executed on 32nd and 33rd day. Behavioral tests were carried out between 09:00 am to 5:00 pm. Mice were relocated to the testing room 20 min before the initiation of the first trial to acquaint it with the environment of the testing room. The temperature of the testing room was well retained at the 25 ± 2 °C. The behavioral tests were carried in

the absence of an investigator and the entire tests were videotaped by a cam and the results were analyzed for final outcomes [33,34].

4.5.3. Morris water maze test

It is used find out the memory and learning of the animal's knowledge about the surrounding and its spatial remembrance. The apparatus used for this procedure has a round pool with 120-cm diameter and a depth of 60 cm. This pool is divided in 4 hypothetical quadrants South, West, East, and North. The trial began on the 27th day and 5 trials were executed each day. The mouse was given only 60 *sec* to find out the hidden platform in each test and an interval of 10 min between the two successive trials was given. The usual time essential by a mouse to arrive at the platform was recorded and an average of 5 trials was presumed as the escape latency of the animal for that day. On the 32nd day of intervention probe test was executed when there was no platform, while the release location/point of the animal was maintained the same as North-East (NE). The spatial learning/memory of the mouse was analyzed by computing the time-spent by the mouse in the same quadrant in which the platform was formerly located. The number of crossings across the earlier platform position was also found out [35,36].

4.5.4. Novel object recognition test

The novel object recognition test used as a modified form of the methodology described in the literature [37]. All the testing procedures were carried out at in a box of (25 cm × 25 cm × 25 cm), daytime at 25 ± 2 °C in the same room. The methodology includes four phases: (1) pre-habituation; (2) habituation; (3) training and (4) testing (Fig. 5). Mice were carried into the testing-room 30–35 min prior to the initiation of the experiment on the first day, to get acquainted with the surroundings. They were allowed for the free exploration of the box without having any objects for five min [37]. Mice were familiarized within the empty box for twenty min on the second and third days. On the fourth day, every mouse was exposed to a trial of training followed by a testing trial. In the training trial, 2 objects were located oppositely to each other inside the box at a similar space from the adjacent corner [38]. The mice could discover the objects for 10 min and then brought back to home cages. After an hour the mice were located again to the same experimental box, whereas one of the two familiarized objects was substituted by a new/novel object, for the start of a 10 min testing phase [39]. The behavior of the mouse was recorded with a video-came. Recognition index can be calculated by the formula given below;

Recognition Test = [Time spent with novel object/Time spent with object 1+novel object] × 100

4.6. Statistics

All numerical values were given as mean ± SEM. Column statistic was used to compare the results and level of significance was set at $p < 0.05$.

Acknowledgements

This research work is partially supported by the COMSATS University Islamabad, Abbottabad campus under the funding project # 16-60/CRGP/CIIT/ABT/14/635 and partly by the International Research Support Initiative Program (IRSIP) higher education commission Islamabad, Pakistan for abroad visit to the MSU, USA.

Appendix A. Supplementary material

Supplementary data to this article can be found online at https://doi.org/10.1016/j.bioorg.2019.102936.

References

[1] W.W. Barker, C.A. Luis, A. Kashuba, M. Luis, D.G. Harwood, D. Loewenstein, Relative frequencies of Alzheimer disease, lewy body, vascular and frontotemporal dementia, and hippocampal sclerosis in the State of Florida Brain Bank, Alzheimer, Dis. Assoc. Disord. 16 (2002) 203–212.
[2] A.K. Ghosh, E.R. Mannhold, H. Kubinyi, G. Folkers, G.F. Chiba, Aspartic acid proteases as therapeutic targets, first ed., Wiley-VCH, 2010.
[3] R. Vassar, B.D. Bennett, S. Babu-Khan, S. Kahn, E.A. Mendiaz, P. Denis, Beta-secretase cleavage of Alzheimer's amyloid precursor protein by the transmembrane aspartic protease BACE, Science 286 (1999) 735–741.
[4] D.S. Wang, D.W. Dickson, J.S. Malter, β-Amyloid degradation and Alzheimer's disease, J. Biomed. Biotechnol. (2006) 1–12, https://doi.org/10.1155/JBB/2006/58406.
[5] C.P. Ferri, M. Prince, M.C. Brayne, C.H. Brodaty, L. Fratiglioni, M. Ganguli, Global prevalence of dementia: a Delphi consensus study, Lancet 2005 (366) (2005) 2112–2117.
[6] R.J. O'Brien, P.C. Wong, Amyloid precursor protein processing and Alzheimer's disease, Annu. Rev. Neurosci. 34 (2011) 185–204.
[7] C.A. Taft, C.H.T. de Paula Da, Silva, New Developments in Medicinal Chemistry, Bentham Science Publishers, Amazon, France, 2014.
[8] S. Sinha, J.P. Anderson, R. Barbour, G.S. Basi, R. Caccavello, D. Davis, M. Doan, H.F. Dovey, N. Frigon, J. Hong, K. Jacobson-Croak, N. Jewett, P. Keim, J. Knops, I. Lieberburg, M. Power, H. Tan, G. Tatsuno, J. Tung, D. Schenk, P. Seubert, S.M. Suomensaari, S. Wang, D. Walker, J. Zhao, L. McConlogue, V. John, Purification and cloning of amyloid precursor protein beta-secretase from human brain, Nature 402 (1999) 537–540.
[9] L. Hong, G. Koelsch, X. Lin, S. Wu, S. Terzyan, A.K. Ghosh, X.C. Zhang, J. Tang, Structure of protease domain of memapsin 2 (beta-secretase) complexed with inhibitor, Science 290 (2000) 150–153.
[10] D. Shuto, S. Kasai, T. Kimura, P. Liu, K. Hidaka, T. Hamada, S. Shibakawa, Y. Hayashi, C. Hattori, B. Szabo, S. Ishiura, Y. Kiso, KMI-008, a novel beta-secretase inhibitor containing a hydroxymethylcarbonyl isostere as a transition-state mimic: design and synthesis of substrate-based octapeptides, Bioorg. Med. Chem. Lett. 13 (2003) 4273–4276.
[11] S.J. Stachel, C.A. Coburn, S. Sankaranarayanan, E.A. Price, G. Wu, M. Crouthamel, B.L. Pietrak, Q. Huang, J. Lineberger, A. Espeseth, L. Jin, J. Ellis, M.K. Holloway, S. Munshi, T. Allison, D. Hazuda, A.J. Simon, S.L. Graham, J.P. Vacca, Macrocyclic inhibitors of beta-secretase: functional activity in an animal model, J. Med. Chem. 49 (2006) 6147–6150.
[12] P. Zhou, Y. Li, Y. Fan, Z. Wang, R. Chopra, A. Olland, Y. Hu, R.L. Magolda, M. Pangalos, P.H. Reinhart, M.J. Turner, J. Bard, M.S. Malamas, A.J. Robichaud, Pyridinyl aminohydantoins as small molecule BACE1 inhibitors, Bioorg. Med. Chem. Lett. 20 (2010) 2326–2329.
[13] R. Godemann, J. Madden, J. Krämer, M. Smith, U. Fritz, T. Hesterkamp, T.J. Barker, S. Höppner, D. Hallett, A. Cesura, A. Ebneth, J. Kemp, Fragment-based discovery of BACE1 inhibitors using functional assays, Biochemistry 48 (2009) 10743–10751.
[14] D.k. Lahiri, B. Maloney, J.M. Long, N.H. Greig, Lessons from a BACE1 inhibitor trial: Off-site but not off base, Alzheimers, Dement 10 (2014) S411–S419.
[15] M. Citron, Secretase as a target for the treatment of Alzheimer's disease, J. Neurosci. Res. 70 (2002) 373–379.
[16] M.E. Kennedy, W. Wang, L. Song, J. Lee, L. Zhang, G. Wong, Measuring human beta secretase (BACE1) activity using homogeneous time-resolved fluorescence, Anal. Biochem. 319 (2003) 49–55.
[17] D. Oehlrich, H. Prokopcova, H.J.M. Gijsen, The evolution of amidine-based brain penetrant BACE1 inhibitors, Bioorganic. Med. Chem. Lett. 24 (2014) 2033–2045.
[18] J. Gasteiger, M. Marsili, Iterative partial equalization of orbital electronegativity—a rapid access to atomic charges, Tetrahedron 36 (1980) 3219–3228.
[19] H. Cheng, K.S. Vetrivel, P. Gong, X. Meckler, A. Parent, G. Thinakaran, Mechanisms of disease: new therapeutic strategies for Alzheimer's disease targeting APP processing in lipid rafts, Nat. Clin. Pract. Neuro. 3 (2007) 374–382.
[20] W. Sherman, T. Day, M.P. Jacobson, R.A. Friesner, R. Farid, Novel procedure for modeling ligand/receptor induced fit effects, J. Med. Chem. 49 (2006) 534–555.
[21] O. Trott, A.J. Olson, AutoDock Vina: improving the speed and accuracy of docking with a new scoring function, efficient optimization, and multithreading, J. Comput. Chem. 31 (2010) 455–461.
[22] J. Karsten, L. Tagmose, M. Marigo, 2-amino-3-fluoro-3-(fluoromethyl)-6-methyl-6-phenyl-3, 4, 5, 6-tetrahydropyridines as BACE1 inhibitors, U.S. Patent Application No. 10/011,596.
[23] F. Leroux, P. Jeschke, M. Schlosser, α-fluorinated ethers, thioethers and amines: anomerically biased species, Chem. Rev. 105 (2005) 827–856.
[24] W.K. Hagmann, The many roles for fluorine in medicinal chemistry, J. Med. Chem. 51 (2008) 4359–4369.
[25] C.A. Lipinski, Lead and drug-like compounds: the rule-of-five revolution, Drug. Discov. Today. Technol. 1 (2004) 337–341.
[26] C. Exley, Molecular mechanism of aluminium-induced Alzheimer's disease? J. Inorg. Biochem. 76 (1999) 133–140.
[27] N. Jones, S.M. King, Influence of circadian phase and test illumination on preclinical models of anxiety, Physiol. Behav. 72 (2001) 99–106.
[28] N.P. Van Goethem, K. Rutten, F.J. van der Staay, L.A.W. Jans, S. Akkerman, H.W.M. Steinbusch, Object recognition testing: rodent species, strains, housing conditions, and estrous cycle, Behav. Brain. Res. 232 (2012) 323–334.
[29] D. Santos-Martins, S. Forli, M.J. Ramos, A.J. Olson, AutoDock4Zn: An improved AutoDock force field for small-molecule docking to zinc metalloproteins, J. Chem. Inf. Model. 54 (2014) 2371–2379.

[30] S. Vilar, G. Cozza, S. Moro, Medicinal chemistry and the molecular operating environment (MOE): application of QSAR and molecular docking to drug discovery, Curr. Top. Med. Chem. 8 (2008) 1555–1572.
[31] B. Chu, F. Liu, L. Li, C. Ding, K. Chen, Q. Sun, A benzimidazole derivative exhibiting antitumor activity blocks EGFR and HER2 activity and upregulates DR5 in breast cancer cells, Cell. Death. Dis. 6 (2015) e1686.
[32] C.X. Zhang, G.J. Zheng, F.Q. Bi, Y.L. Li, A simple and efficient synthesis of the valsartan, Chinese. Chem. Lett. 19 (2008) 759–761.
[33] P. Bamborough, J.A. Christopher, G.J. Cutler, M.C. Dickson, G.W. Mellor, J.V. Morey, 5-(1H-Benzimidazol-1-yl)-3-alkoxy-2-thiophenecarbonitriles as potent, selective, inhibitors of IKK-ε kinase, Bioorganic. Med. Chem. Lett. 16 (2006) 6236–6240.
[34] O. René, A. Souverneva, S.R. Magnuson, B.P. Fauber, Efficient syntheses of 2-fluoroalkylbenzimidazoles and –benzothiazoles, Tetrahedron. Lett. 54 (2013) 201–204.
[35] K. Bromley-Brits, Y. Deng, W. Song, Morris water maze test for learning and memory deficits in Alzheimer's disease model mice, J. Vis. Exp. 53 (2011) 2920.
[36] A. Mahboob, S.M. Farhat, G. Iqbal, M.M. Babar, S.S. Zaidi, N.S.M. Nabavi, Alpha-lipoic acid-mediated activation of muscarinic receptors improves hippocampus- and amygdala-dependent memory, Brain. Res. Bull. 122 (2016) 19–28.
[37] S. Akkerman, A. Blokland, O. Reneerkens, G.N.P. Van, E. Bollen, H.J.M. Gijselaers, Object recognition testing methodological considerations on exploration and discrimination measures, Behav. Brain. Res. 232 (2012) 335–347.
[38] R.N. Hughes, Neotic preferences in laboratory rodents : Issues, assessment and substrates, Neurosci. Biobehav. Rev. 31 (2007) 441–464.
[39] R. Zhang, G. Xue, S. Wang, L. Zhang, C. Shi, X. Xie, Novel object recognition as a facile behavior test for evaluating drug effects in AβPP/PS1 Alzheimer's disease mouse model, J. Alzheimer's. Dis. 31 (2012) 801–812.